Imaging mass spectrometry: A new technology for the analysis of protein expression in mammalian tissues

MARKUS STOECKLI, PIERRE CHAURAND, DENNIS E. HALLAHAN & RICHARD M. CAPRIOLI
Mass Spectrometry Research Center, Vanderbilt University School of Medicine, Nashville, Tennessee, USA
Correspondence should be addressed to R.M.C.; email: r.caprioli@vanderbilt.edu

The molecular specificity and sensitivity of mass spectrometry (MS) has been employed in a new technology for direct mapping and imaging of biomolecules present in tissue sections. This technology has been developed using matrix-assisted laser desorption/ionization MS (MALDI MS)[1] and has been initially targeted for the analysis of peptides and proteins present on or near the surface of tissue sections[2]. Imaging MS brings a new tool to bear on the problem of unraveling and understanding the molecular complexities of cells. It joins techniques such as immunochemistry and fluorescence microscopy for the study of the spatial arrangement of molecules within biological tissues. Many previous experiments using MS to image samples have focused on the measurement of the distribution of elements and small molecules in biological specimens, including tissue slices and individual cells[3–5]. An extensive review on imaging by MS can be found in the article by Pacholski and Winograd[6].

Technological aspects

For the molecular image analysis, tissue samples can be prepared using several protocols: direct analysis of fresh frozen sections[7–9], individual cells or clusters of cells isolated by laser-capture microdissection or contact blotting of a tissue on a membrane target[10]. In a typical preparation procedure (Fig. 1), we mounted a frozen section of tissue on a stainless steel target plate, coated it with a solution of matrix (for example, sinapinic acid), then dried and introduced into the vacuum inlet of the mass spectrometer (Voyager Elite DE, Applied Biosystems, Framingham, Massachusetts). The instrument was controlled by MS imaging software written in our laboratory[11]. We created molecular images from a raster over the surface of the sample with consecutive laser spots (~25 µm in diameter). The laser position was fixed and the sample plate was repositioned for consecutive spots. Each spot produced a mass spectrum obtained from molecules present within the irradiated area. Typically, each mass spectrum was the average of 50 laser shots acquired using a fast transient recorder PC board (DP211, Acqiris, Geneva, Switzerland). With a laser frequency of 20 Hz, the time cycle was about 2.5 seconds per data point, including acquisition, data download to the computer, data processing and repositioning of the sample stage. A typical data array was 1,000–30,000 spots depending on the desired image resolution, which contains the intensity of ions desorbed at each spot in a molecular weight range of 500 D to over 80 kD. For most tissue sections, we recorded over 200 protein and peptide peaks in the mass spectrum from each spot ablated by the laser. We could produce an MS image or molecular weight-specific map of the sample at any desired molecular weight value. It is commonly possible to generate individual maps to verify the presence, molecular weight and location of proteins. In the fullest extent, from a single raster of a piece of tissue, imaging MS could produce hundreds of image maps each at a discrete molecular weight value.

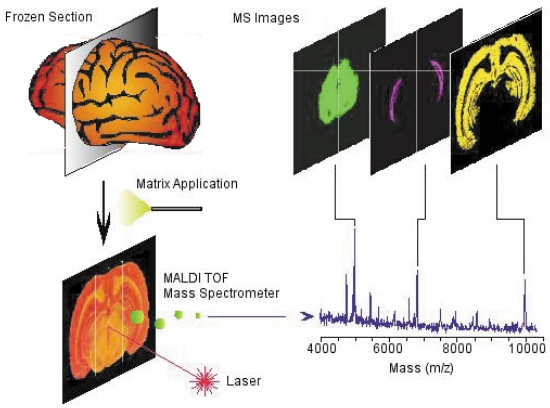

Fig. 1 Methodology developed for the spatial analysis of tissue by MALDI mass spectrometry. Frozen sections are mounted on a metal plate, coated with an UV-absorbing matrix and placed in the mass spectrometer. A pulsed UV laser desorbs and ionizes analytes from the tissue and their m/z values are determined using a time-of-flight analyzer. From a raster over the tissue and measurement of the peak intensities over thousands of spots, mass spectrometric images are generated at specific molecular weight values.

Application to mammalian tissue

We used imaging MS to study normal tissue sections from mouse brain and human brain tumor xenograph sections. These samples contained well-defined regions, many of which had subsets of proteins and peptides in a unique distribution or array. The bilateral symmetry of the brain provides an internal confirmation of the localized distribution of proteins and the homogeneity of the prepared tissue sections. An optical image of the normal mouse brain section fixed on a metal plate and coated with matrix is shown in Fig. 2*a*. We scanned the section by acquiring 170 × 90 spots with a spot-to-spot center distance of 100 µm in each direction. We recorded ions occurring in 82 different mass ranges and created images by integrating the peak areas and plotting the relative values using a color scale. For specific molecular images, we acquired data in a window delimited by two mass-to-charge (m/z) units on either side of the molecular peak. Although many of the protein signals were common to all areas of the brain, some were found to be highly specific for a given brain region. For example, the protein detected at m/z 8258 ± 1 (Fig. 2*b*) was present in the regions of the cerebral cortex and the hippocampus; the protein at m/z 6716 ± 1 (Fig. 2*c*) was localized in the regions of the substantia nigra and medial geniculate nucleus; and the peptide at m/z 2564 ± 1 was in the midbrain (Fig. 2*d*). These ions are $[M+H]^+$ species, and the molecular weights of the compounds were obtained by subtracting the weight of a proton, nominally 1 m/z unit from the

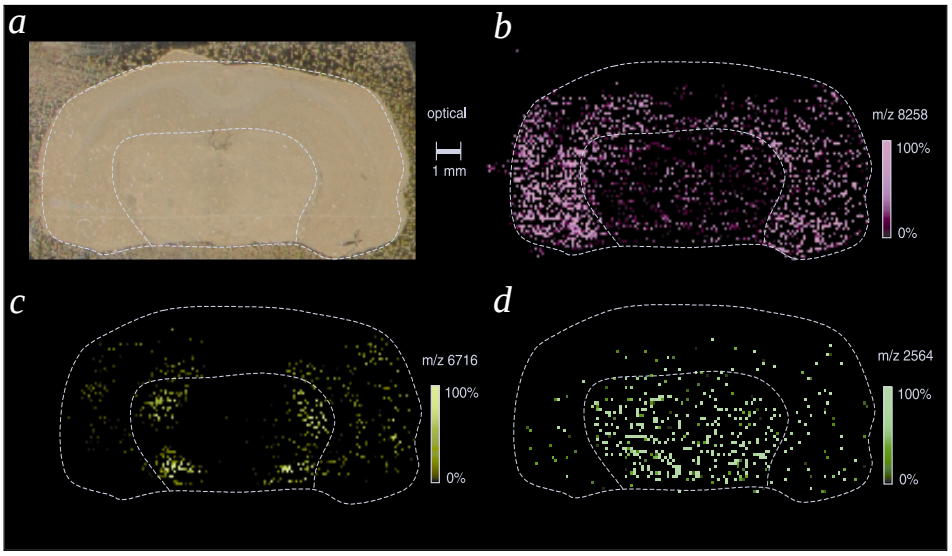

Fig. 2 Mass spectrometric images of a mouse brain section. ***a***, Optical image of a frozen section mounted on a gold-coated plate. ***b***, m/z 8,258 in the regions of the cerebral cortex and the hippocampus. ***c***, m/z 6,716 in the regions of the substantia nigra and medial geniculate nucleus ***d***, m/z 2,564 in the midbrain.

measured m/z value. Identification of the proteins can be done through extraction, HPLC fractionation, proteolysis, mass spectrometric sequencing of one or more of the fragments and protein database searching. This procedure is illustrated below for proteins in tumor sections.

Molecular imaging of tumor sections

One our aims is the molecular analysis and imaging of peptides and proteins in brain tumors, specifically in human glioblastoma. Such an analysis would be an important if not essential part of strategies designed to locate specific proteins that are more highly expressed in tumors and those greatly diminished in expression, relative to normal tissue. Currently, brain tumors account for 2% of all cancer deaths, or about 11,000 deaths annually in the United States. Gliomas account for 50% of all primary brain tumors, with glioblastomas compromising half of those[12].

Here, tumor-bearing tissues were generated by subcutaneous implantation of human glioblastoma cells (D54) into the hind limb of a nude mouse. After tumors grew to about 1 cm in diameter, we surgically removed them from the mouse and immediately froze them using liquid nitrogen. For image analysis, we cut the tumor tissue using a microtome in 12-µm thick sections orthogonal to the point of attachment to normal tissue. Frozen sections were processed following the protocol described above before image analysis by MS.

The optical image of a frozen human glioblastoma section taken immediately following mass spectrometric imaging is shown in Fig. 3*a*. The orientation in the figure is such that the actively growing area of the tumor is at the top of the figure, and the point where the tumor was attached to the healthy tissue at the bottom. The fine line (cross-hatched) pattern on the optical image was produced by laser ablation of the surface during the scan. Mass spectrometric images were produced from a raster over an area of 8.5 mm × 8 mm (image spots 100 µm apart on center). During the scan, we recorded images of ions in 45 mass ranges and the mass spectra were saved for further analysis. Three mass spectrometric images of molecules present in distinct areas of the tumor are shown in Fig. 3*b–d*. In this figure, color is used to represent different ions, with color saturation a function of the relative intensity (see color reference bar). Overall, we detected over 150 different proteins, with many being present in all parts of the tissue. Individual selected proteins were identified as described below. We took three different

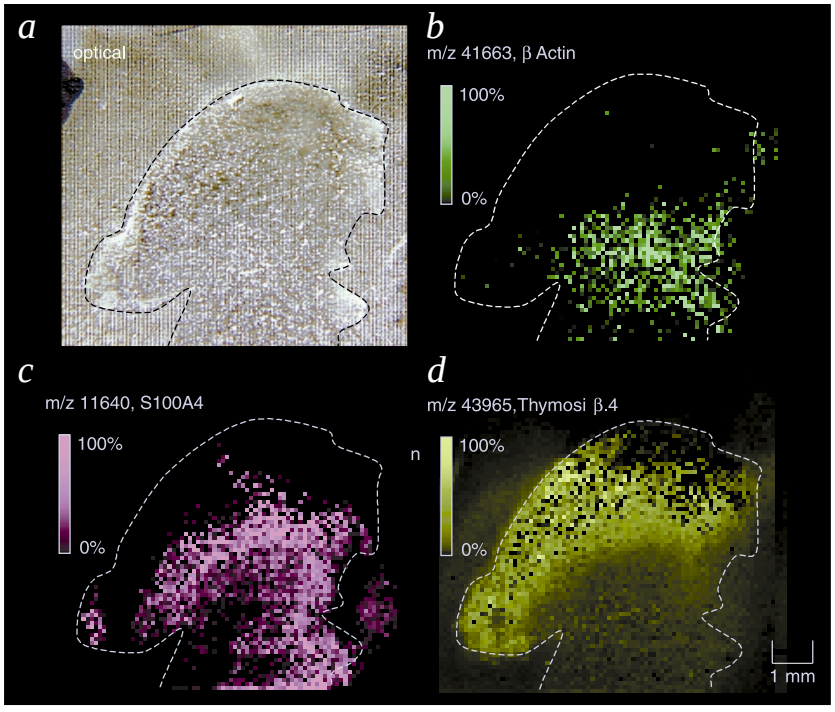

Fig. 3 Selected protein images from a glioblastoma section. ***a***, Human glioblastoma slice mounted on a metal plate, coated with matrix (the lines are from ablation of matrix with the laser). ***b–d***, Mass spectrometric images of proteins showing high concentration in the proliferating area of the tumor (*d*) and other proteins present specifically in the ischemic and necrotic areas (*b* and *c*).

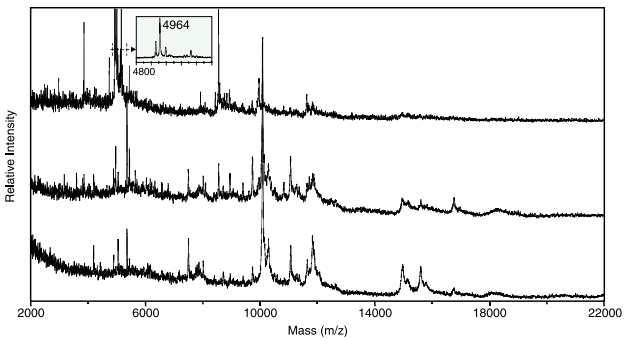

Fig. 4 MALDI mass spectra taken at different locations within a glioblastoma slice (Fig. 3). Over 150 different peaks could be detected, with some of them having a distinct spatial distribution in the tissue. *Top*, distal and most active area of tumor proliferation; *middle*, an ischemic area; *bottom*, a necrotic area of the tumor. The inset shows an expanded portion of the spectrum in the region of thymosin β.4.

mass spectra from different regions of the glioblastoma during the scan (Fig. 4). These spectra clearly show differences in protein expression in different parts of the tumor.

The proliferating area of the tumor was of particular interest with many proteins being expressed at higher levels relative to normal tissue. For example, the protein of molecular weight 4,964 (Fig. 3*d*) is localized only in the outer area of the tumor. Other proteins, such as that of molecular weight 41,662 (Fig. 3*b*), were localized in the necrotic area. In addition, other proteins were localized in the ischemic area between the necrotic center and proliferating periphery, as shown for the protein with a molecular weight of 11,639. To identify the mapped proteins, we made an extract of the appropriate portion of the glioblastoma tissue, and then fractionated the proteins by HPLC. The UV chromatogram of such an extract is shown in Fig. 5. The on-line mass spectrometric analysis (Ion Trap, Finnigan Company, San Jose, California) performed using electrospray ionization MS easily permitted localization of the fraction containing the proteins of interest. For example, one of the proteins of molecular weight 4,964 eluted at 28.35 min in the chromatogram. We spotted a sample of this fraction onto a MALDI target plate and performed an on-target digestion by trypsin. We analyzed the digest by MALDI MS followed by a database search in SwissProt using the software 'MoverZ' (ProteoMetrics, New York, New York). Thymosin β.4 (Tβ.4) was found to match the digest data precisely. The sequence analysis of the amino-terminal peptide confirmed the identification of the protein as Tβ.4 in this human glioblastoma xenograft. Increased expression of Tβ.4 has been reported in a variety of different tumors[13]. The localization of Tβ.4 in the proliferating area of the tumor correlates with previous findings of higher levels of Tβ.4 in embryonic/neoplastic tissue compared with normal/benign tissue[14]. One of the known activities of this immunoregulatory peptide is its ability to sequester cytoplasmic monomeric actin[15]. Moreover, actin filaments have been shown to change into clump formation in apoptosis induced by antitumor drugs, a process thought to be the result of decreased Tβ.4 concentrations[16].

We also observed the increased expression of Tβ.4 in other tumors as well. For example, in some mouse models of prostate cancer, high levels of this protein have been found using imaging MS. To confirm the identification, we generated a fragment ion spectrum (MS/MS analysis) using an electrospray quadrupole TOF mass spectrometer (Q-Star, Applied Biosystems/SCIEX, Foster City, California) from one of the tryptic fragments. The MS/MS spectrum of the N-terminal tryptic peptide obtained from a similar digest of Tβ.4 purified from a mouse with prostate cancer is shown in Fig. 6. Fragment ions were matched by identifying portions of the y and b ion series[17], covering the complete sequence of the peptide. This spectrum confirmed the presence of Tβ.4 in mouse models of prostate cancer. Furthermore, from the MS/MS spectrum, the presence of an acetyl group at the N-terminal end of the Tβ.4 peptide was confirmed. The protein of molecular weight 11,639 ± 2 (Fig. 3*c*) was similarly identified as S100 calcium-binding protein A4 (S100A4), and the protein of measured molecular weight 41,659 ± 4 to be cytoplasmic actin.

Discussion

The identification of specific tumor markers, for example Tβ.4, in the proliferating area of the tumors demonstrates the potential of this technique to be used in intra-operative assessment of the surgical margins of tumors. Currently, frozen sections and light microscopy are required for rapid decisions, but are, at times, inaccurate[18,19]. There is presently a need to develop technology to improve the accuracy of such decisions[20,21]. For example, cancer invasion into muscle indicates that more extensive surgery or adjuvant therapy is needed[22,23] and intra-operative diagnosis of central nerve system neoplasia is required for surgical management[24–26]. Clinical validation will determine the usefulness of imaging MS to demonstrate these pathologic criteria accurately for more aggressive management of cancer.

Beyond the application of imaging MS to brain cancer research, we are currently using this technology to study prostate and colon cancer development and progression. In both cases, numerous tumor-specific markers have been identified and specifically localized within the tumors. Protein profiling and imaging MS are also proving to be of prime importance in our current research aiming at a better understanding of prostate development. Overall, imaging MS can be a valuable molecular tool in a wide variety of studies and applications involving animal tissues.

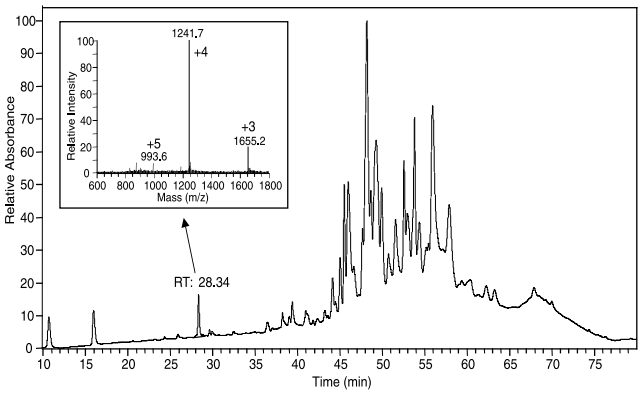

Fig. 5 UV chromatogram of a LC separation on a glioblastoma xenograft extract. The analyte of molecular weight 4,964 was detected by online electrospray mass spectrometry (inset shows mass spectrum) at a retention time of 28.3 min.

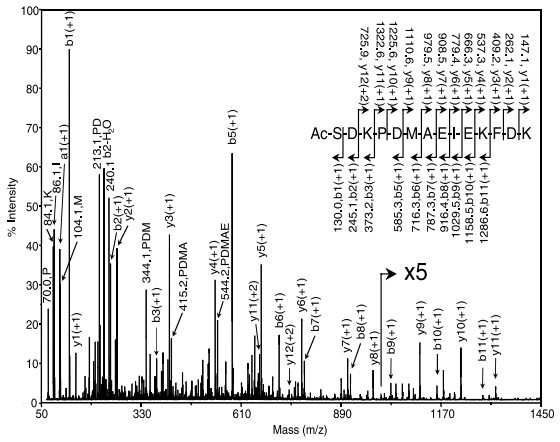

Fig. 6 The mass spectrometric analysis by electrospray MS/MS of the N-terminal tryptic fragment of Tβ.4. The complete sequence of the fragment was confirmed from the mass spectrometric data.

Acknowledgments

We thank S. Schroeter, E. Sierra-Rivera, B. DaGue and Darell Bigner for help with this study. This work was supported by NIH grants GM 58008 (to R.M.C.), CA 58506 (to D.H.) and C.A. 70937 (to D.H.).

1. Karas, M., Bachmann, D., Bahr, U. & Hillenkamp, F. Matrix-assisted ultraviolet-laser desorption of nonvolatile compounds. *Int. J. Mass Spectrom. Ion Process.* **78**, 53–68 (1987).
2. Caprioli, R.M., Farmer, T.B. & Gile, J. Molecular imaging of biological samples: Localization of peptides and proteins using MALDI-TOF MS. *Anal. Chem.* **69**, 4751–4760 (1997).
3. Valaskovic, G.A. & Morrison, G.H. Quantitative imaging ion microscopy — a short review. *Scanning Microscopy* **6**, 305–318 (1992).
4. Levisetti, R. *et al.* Imaging-SIMS (secondary-ion mass-spectroscopy) studies of advanced materials. *Scanning Microsc.* **7**, 1161–1172 (1993).
5. Todd, P.J., McMahon, J.M., Short, R.T. & McCandlish, C.A. Organic SIMS of biological tissue. *Anal. Chem.* **69**, 529A–535A (1997).
6. Pacholski, M.L. & Winograd, N. Imaging with mass spectrometry. *Chem. Rev.* **99**, 2977–3005 (1999).
7. Li, K.W. *et al.* Direct peptide profiling by mass spectrometry of single identified neurons reveals complex neuropeptide-processing pattern. *J. Biol. Chem.* **269**, 30288–30292 (1994).
8. Jimenez, C.R. *et al.* Direct mass spectrometric peptide profiling and sequencing of single neurons reveals differential peptide patterns in a small neuronal network. *Biochemistry* **37**, 2070–2076 (1998).
9. Moroz, L.L., Gillette, R. & Sweedler, J.V. Single-cell analyses of nitrergic neurons in simple nervous systems. *J. Exp. Biol.* **202**, 333–341 (1999).
10. Chaurand, P., Stoeckli, M. & Caprioli, R.M. Direct profiling of proteins in biological tissue sections by MALDI mass spectrometry. *Anal. Chem.* **71**, 5263–5270 (1999).
11. Stoeckli, M., Farmer, T.B. & Caprioli, R.M. Automated mass spectrometry imaging with a matrix-assisted laser desorption ionization time-of-flight instrument. *J. Am. Soc. Mass Spectrom.* **10**, 67–71 (1999).
12. Nelson, D.F., McDonald, J.V., Lapham, L.W., Quazi, R. & Rubin, P. Central nervous system tumors. in *Clinical Oncology: A Multidisciplinary Approach for Physicians and Students* (ed. Rubin, P.) 617–644 (WB Saunders, Philadelphia, 1993).
13. Paciucoi, R. *et al.* Isolation of plasminogen activator, cathepsin H, and non-specific cross-reacting antigen from SK-PC-1 pancreas cancer cells using subtractive hybridization. FEBS Lett. **385**, 72–76 (1996).
14. Hall, A.K. Differential expression of thymosin genes in human tumors and in the developing human kidney. *Int. J. Cancer* **48**, 672–677 (1991).
15. Sun, H.Q., Kwiatowska, K., Yin, H.L. Actin monomer binding proteins. Curr. Opin. Cell Biol. **7**, 102–110 (1995).
16. Iguchi, K. *et al.* Decreased thymosin β.4 in apoptosis induced by a variety of antitumor drugs. *Biochem. Pharmacol.* **57**, 1105–1111 (1999).
17. Roepstorff, P. Proposal for a common nomenclature for sequence ions in mass spectra of peptides. *Biomed. Mass Spectrom.* **11**, 601 (1984).
18. Turner, R.R., Hansen, N.M., Stern, S.L. & Giuliano, A.E. Intra-operative examination of the sentinel lymph node for breast carcinoma staging. *Am. J. Clin. Pathol.* **112**, 627–634 (1999).
19. Gibbs, J.F., Huang, P.P., Zhang, P.J., Kraybill, W.G. & Cheney, R. Accuracy of pathologic techniques for the diagnosis of metastatic melanoma in sentinel lymph nodes. *Ann. Surg. Oncol.* **6**, 699–704 (1999).
20. Richter, T., Nahrig, J., Komminoth, P., Kowolik, J. & Werner, M. Protocol for ultrarapid immunostaining of frozen sections. *J. Clin. Pathol.* **52**, 461–463 (1999).
21. Wang, H.W., Willis, J., Canto, M.I.F., Sivak, M.V. & Izatt, J.A. Quantitative laser scanning confocal autofluorescence microscopy of normal, premalignant, and malignant colonic tissues. *IEEE Trans. Biomed. Eng.* **46**, 1246–1252 (1999).
22. Cheng, L., Neumann, R.M., Weaver, A.L., Spotts, B.E. & Bostwick, D.G. Predicting cancer progression in patients with stage T1 bladder carcinoma. *J. Clin. Oncol.* **17**, 3182–3187 (1999).
23. Longacre, T.A. & Hendrickson, M.R. Diffusely infiltrative endometrial adenocarcinoma — an adenoma malignum pattern of myoinvasion. *Am. J. Surg. Pathol.* **23**, 69–78 (1999).
24. Shah, A.B., Muzumdar, G.A., Chitale, A.R. & Bhagwati, S.N. Squash preparation and frozen section in intra-operative diagnosis of central nervous system tumors. *Acta Cytologica* **42**, 1149–1154 (1998).
25. Silbergeld, D.L. & Chicoine, M.R. Isolation and characterization of human malignant glioma cells from histologically normal brain. *J. Neurosurg.* **86**, 525–531 (1997).
26. Firlik, K.S., Martinez, A.J. & Lunsford, L.D. Use of cytological preparations for the intra-operative diagnosis of stereotactically obtained brain biopsies: A 19-year experience and survey of neuropathologists. *J. Neurosurg.* **91**, 454–458 (1999).

Methods

Tissue preparation. 12-μm sections were cut from a frozen mouse brain on a Leica CM 3000 cryostat at –15 °C and directly picked up onto a gold-coated stainless steel plate. The sections were immediately transferred to a cold room (4 °C), where 10 μl of matrix (sinapinic acid, 10 mg/ml in acetonitrile/0.05% trifluoroacetic acid 50:50) were deposited with a pipette in a line adjacent to the tissue and mechanically spread over the tissue using a small plastic spatula. After air-drying for 45 min, the sections were dried for 2 h in a desiccator before mass spectrometric analysis. This application technique results in formation of crystals of the organic matrix on the surface of the tissue while minimizing the spreading of sample molecules.

Glioblastoma extraction and protein fractionation by HPLC. A portion of the glioblastoma (82 mg) was immersed in 500 μl extraction buffer (0.25 M sucrose, 0.01 M Tris-HCl and inhibitor mix; (Roche Molecular Biochemicals, Switzerland), homogenized using a Duall homogenizer and centrifuged 3 times (10 min at 680*g*, 10 min at 10,000*g* and 1 h at 55,000*g*), each time transferring the soluble fraction to a new tube. The final fraction (50 μl) was separated over a C4 microbore column (Vydac, Hesperia, California), samples were collected and the separation run was recorded with a UV detector set at 214 nm. Solvent A was 0.1 trifluoro acetic acid and solvent B was 95% acetonitrile, 5% water and 0.1% trifluoro acetic acid. A flow rate of 200 μl/min was used with a gradient of 5 min at 5% B, then in 55 min to 60% B, then in 10 min to 100% B, and finally 5 min at 100% B.

On-target digestion by trypsin. For this procedure, the sample (2 μl) was placed on the target and allowed to dry before adding digest solution (2 μl, 20 nM bovine trypsin, sequencing-grade, (Roche Molecular Biochemicals), and 50 mM ammonium hydrogen carbonate). The plate was kept at 37 °C for 30 min while adding water to maintain the volume. After drying the sample, 2 μl of a saturated α-cyano-4-hydroycinnamic acid (Sigma) solution in 50:50 acetonitrile and 0.1% trifluoro acetic acid (2 μl) was added as a MALDI matrix.